Hindawi Publishing Corporation
Journal of Nanomaterials
Volume 2011, Article ID 186528, 5 pages
doi:10.1155/2011/186528

Research Article

Hydrothermal Synthesis of Sb_2S_3 Nanorods Using Iodine via Redox Mechanism

Abdolali Alemi,[1] Sang Woo Joo,[2] Younes Hanifehpour,[1,2] Aliakbar Khandar,[1] Ali Morsali,[3] and Bong-Ki Min[4]

[1] *Department of Inorganic Chemistry, Faculty of Chemistry, University of Tabriz, Tabriz 51664, Iran*
[2] *WCU Nano Research Center, School of Mechanical Engineering, Yeungnam University, Gyeongsan 712-749, Republic of Korea*
[3] *Department of Chemistry, Faculty of Sciences, Tarbiat Modares University, Tehran 14115-175, Iran*
[4] *Center for Research Facilities, Yeungnam University, Gyongsan 712-749, Republic of Korea*

Correspondence should be addressed to Sang Woo Joo, swjoo@yu.ac.kr

Received 24 March 2011; Accepted 2 May 2011

Academic Editor: Zhi Li Xiao

Crystalline antimony sulfide (Sb_2S_3) with nanorods morphology was successfully prepared via hydrothermal method by the reaction of elemental sulfur, antimony, and iodine as starting materials with high yield at 180°C for 24 h. Using oxidation reagent like iodine as an initiator of redox reaction to prepare Sb_2S_3 is reported for first time. The powder X-ray diffraction pattern shows the Sb_2S_3 crystals belong to the orthorhombic phase with calculated lattice parameters, $a = 1.120$ nm, $b = 1.128$ nm, and $c = 0.383$ nm. The quantification of energy-dispersive X-ray spectrometry analysis peaks gives an atomic ratio of 2 : 3 for Sb : S. TEM and SEM studies reveal the appearance of the as-prepared Sb_2S_3 is rodlike which is composed of nanorods with the typical width of 50–140 nm and length of up to 4 μm. The PL emission indicates that band gap of Sb_2S_3 is around 2.50 ev, indicating a considerable blue shift relative to the bulk. A formation mechanism of Sb_2S_3 nanostructure is proposed.

1. Introduction

Antimony sulfide, a layer-structured direct-band-gap semiconductor with orthorhombic crystal structure, is an important semiconductor with high photosensitivity and high thermoelectric power [1]. In the past few years, main-group metal chalcogenides such as A_2B_3 (where A = As, Sb, Bi and B = S, Se, Te) as significant semiconductors have received ever-increasing attention. Due to its good photoconductivity, Sb_2S_3 has received significant attention for potential application in solar energy conversion [2]. It has also been used in switching devices [3], thermoelectric cooling technologies, optoelectronics in the IR region [4, 5], microwave devices [6], and television cameras [7]. Sb_2S_3 exists in two forms: orange amorphous phase and black orthorhombic modification with a ribbon-like polymeric structure along the [001] direction as building blocks [8]. Each Sb atom and each S atom are bonded to three atoms of the opposite kind within the ribbon-like polymeric structure, forming interlocking SbS_3 and SSb_3 pyramids. Consequently, amorphous Sb_2S_3 tends to crystallize into one-dimensional shape to support the stronger intrachain covalent bonds over the relatively weak secondary interchain interaction, during the period of crystallization and lattice arrangement, as what is found in chain-structured trigonal selenium [9]. Over the past two decades, many methods have been employed to prepare Sb_2S_3 including thermal decomposition [10], solvothermal reaction [11, 12], microwave irritation [13], vacuum evaporation [2], and other chemical reaction approaches. Besides an elemental reaction, Sb_2S_3 can be prepared by chemical routes, such as sodium thiosulfate and thioacetamide, ammonium sulfide, and thiourea, as well as with complex agents in aqueous or nonaqueous solution. Li et al. [14] have reported a hydrothermal growth of Sb_2S_3 nanorods without the existence of catalysts or templates. In recent years, the solvothermal method has been applied to synthesize Sb_2S_3

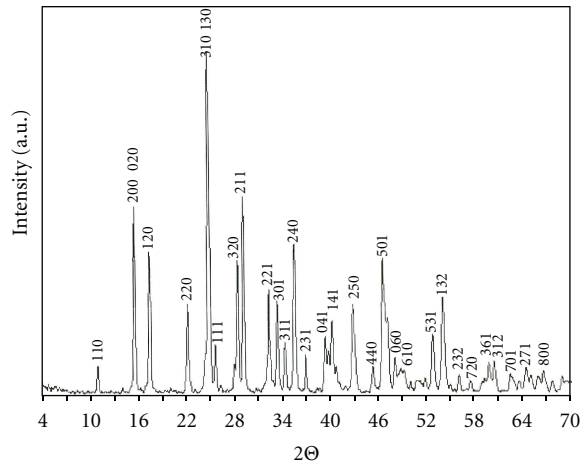

Figure 1: XRD patterns of the Sb_2S_3 nanorods synthesized at 180°C for 24 h.

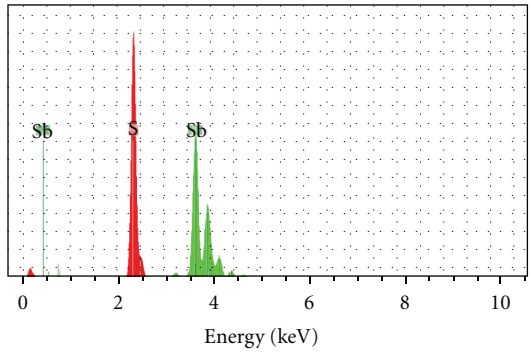

Figure 2: EDX patterns of the Sb_2S_3 nanorodssynthesized at 180°C for 24 h.

nanoparticles, nanorods, and microtubular Sb_2S_3 crystals. Polygonal bulk tubular Sb_2E_3 (E = S, Se) crystals and stibnite nanorods were prepared via the solvothermal route by Zheng et al. [15] and Qian et al. [16], respectively. However, in these methods, the reaction temperature was usually high and the products were usually impure. Therefore, the development of facile, mild, and effective methods for creating novel architectures based on nanorods/submicrometer-sized rods or nanoparticles still remains a great challenge. Recently, there has been a strong trend towards the application of solution chemical synthesis techniques to materials preparation, in which the particle size and distribution, phase homogeneity, and morphology of materials could be well controlled [17]. In this study, Sb_2S_3 nanorods were prepared via hydrothermal method by using antimony, sulfur, and iodine in elemental form as raw materials. This is a new route for the preparation of Sb_2S_3 nanomaterials. Elemental iodine is an oxidizing irritant and acts as an initiator material in the reaction of elemental antimony and sulfur. Without iodine, no reaction is occurred. Using oxidation reagent like iodine as an initiator of redox reaction to prepare Sb_2S_3 is reported for the first time.

2. Experimental

All the reagents were of analytical grade and were used without further purification. In a typical procedure, 2 mmoL Sb, 3 mmoL S, and 1 mmoL I_2 were added to 50 mL distilled water and stirred well for 20 min at room temperature. Then, the mixture was transferred into a 100 mL Teflon-lined autoclave. The autoclave was sealed, maintained at 180°C for 24 h, and cooled at room temperature, naturally. The black precipitate was filtered and washed with dilute chloride acid and water. Yields for the products were 95%. Finally, the obtained sample was dried at room temperature and used for characterization. The best conditions for this reaction are pH 12, temperature 180°C, and time of reaction 24 h.Under other conditions, some impurity is seen in XRD patterns and EDS related to unreacted raw elements or formation of antimony oxides.The crystal structure of the product was characterized by X-ray diffraction (XRD D500 Simens) with CuKα radiation (λ = 1.5418 Å).The morphology of materials were examined by a scanning electron microscope SEM (Hitachi S-4200).The HRTEM image and SAED pattern were recorded by a Cs-corrected high-resolution TEM (JEM-2200FS, JEOL) operated at 200 kV. The TEM sample was prepared by using an FIB (Helios Nanolab, FEI). Elemental analysis was carried out using a linked ISIS-300, Oxford EDS (energy dispersion spectroscopy detector).

3. Results and Discussion

Figure 1 shows the XRD pattern of the as-prepared Sb_2S_3. All the peaks in the pattern can be indexed to an orthorhombic phase with lattice parameters a = 1.122 nm, b = 1.128 nm and c = 0.384 nm. The intensity and positions of the peaks are in good agreement with the values reported in the literature (JCPDS card File : 42-1393). No characteristic peaks are observed for other impurities such as antimony oxides.

In order to further confirm the chemical compositions of these nanomaterials, elemental composition analysis was performed by EDXS. Figure 2 shows a typical EDXA spectrum recorded on single crystals, whose peaks are assigned to Sb and S. The atom ratio of Sb and S are 2 : 3 according to EDXA. This data indicates that we have obtained pure Sb_2S_3 single crystals.

The morphology of as-prepared Sb_2S_3 at 180°C and 24 h was examined by SEM indicating the length of nanorods up to 4 μm and 50–140 nm as diameter (Figure 3).

Figure 4(a) shows TEM image of as-prepared Sb_2S_3 nanorods. Also, the typical HRTEM image recorded from the same nanorods is shown in Figure 4(b). The crystal lattice fringes are clearly observed, and average distance between the neighboring fringes is 0.79 nm, corresponding to the [110] plane lattice distance of orthorhombic-structured Sb_2S_3, which suggests that Sb_2S_3 nanorods grow along the [10-1] direction. The SAED pattern of the nanorods indicates its single-crystal nature and long axis [10-1].

To explain the synthesis process, possible chemical reaction involved in the synthesis of Sb_2S_3 could be assigned to iodine and antimony standard electrode potential values.

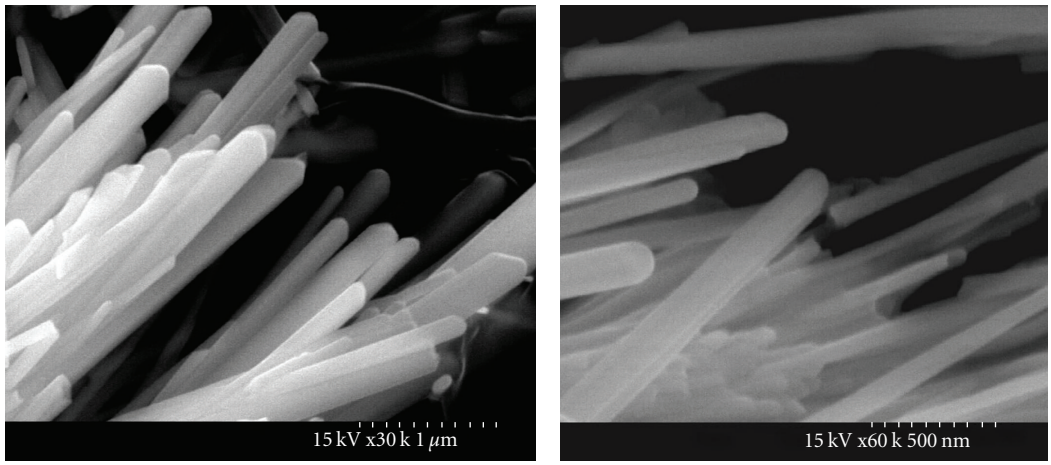

(a) (b)

Figure 3: SEM images of the Sb_2S_3 nanorodsin (a) low and (b) high magnificationssynthesized at 180°C and 24 h.

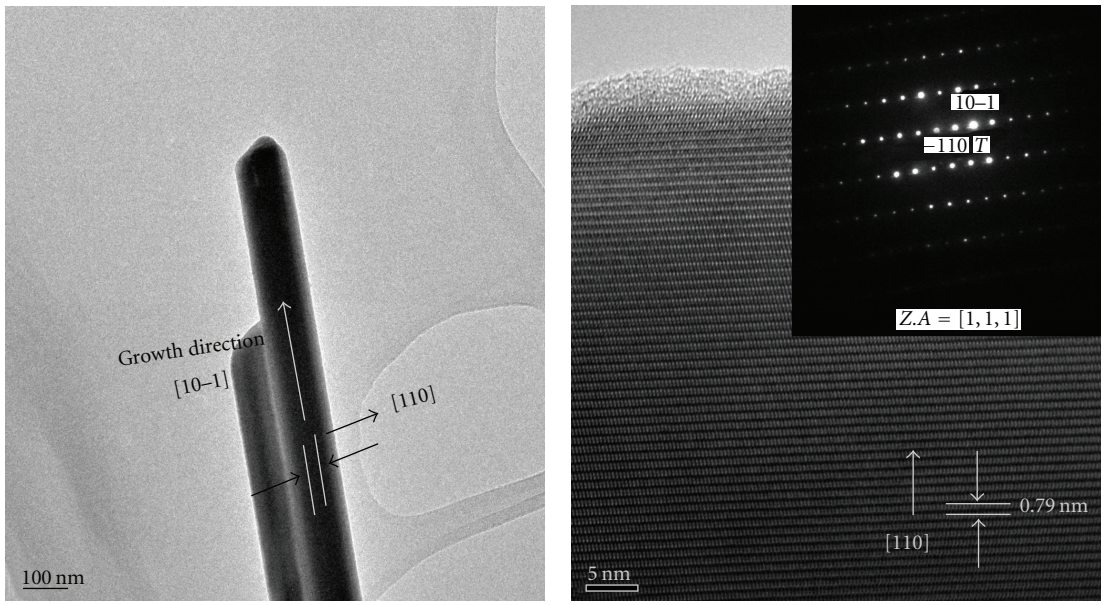

(a) (b)

Figure 4: (a) TEM image of the Sb_2S_3 nanorods synthesized at 180°C and 24 h (b) HRTEM image and SAED (insert) of the Sb_2S_3 nanorods. The SAED zone axis is [111].

Considering the values of standard electrode potentials of Sb^{3+}/Sb ($E_0 = 0.20\,V$) and I_2/I^- ($E_0 = 0.54\,V$), the oxidation reaction between Sb and I_2 is possible

$$Sb^{3+} + 3e \longrightarrow Sb \quad E_0 = 0.20\,V \tag{1}$$

$$I_2 + 2e \longrightarrow 2I^- \quad E_0 = 0.54\,V \tag{2}$$

In terms of electrochemistry, since difference of cathodic and anodic standard electrode potentials values is positive, this redox reaction can occur. In aqueous solution, Iodine and I^- form complex of $I_3{}^-$ which dissolve in water and makes a yellowish solution. The existence of I^- was examined by the formation of red precipitate of Hg_2I_2

$$I_2 + I^- \leftrightarrows I_3{}^- \tag{3}$$

Disproportion of sulfur in this solution is another possibility. Besides the nature of sulfur, the temperature and pressure of autoclave help to disproportion sulfur

$$S + H_2O \longrightarrow SO_4{}^{2-} + S^{2-} \tag{4}$$

Because the precipitate of Sb_2S_3 has a great stability ($Ksp = 1.7 \times 10^{-97}$), the black precipitate of Sb_2S_3 is formed as soon

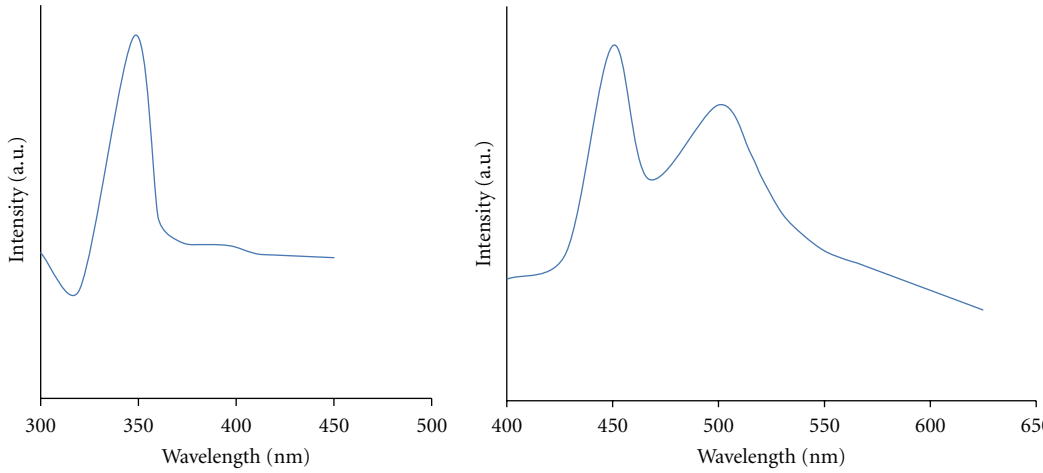

Figure 5: (a) Excitation spectra and (b) emission spectra of Sb_2S_3 nanorods synthesized at 180°C and 24 h.

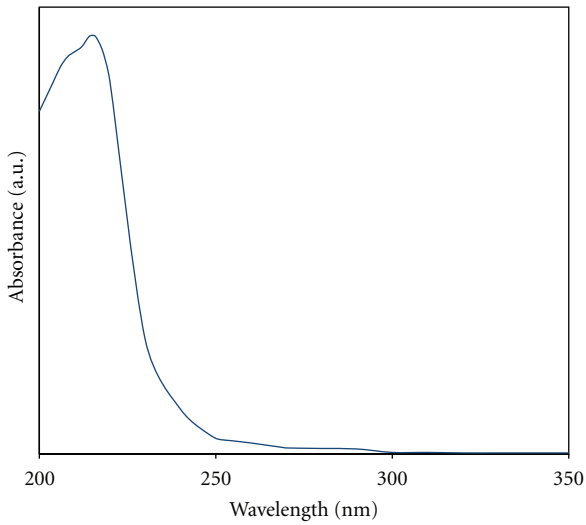

Figure 6: UV/Vis spectra of Sb_2S_3 nanorods synthesized at 180°C and 24 h.

as S^{2-} is produced. Adding Ba^{2+} to the above solution results in white precipitate of $BaSO_4$

$$Sb^{3+} + S^{2-} \longrightarrow Sb_2S_3 \quad Ksp = 1.7 \times 10^{-97} \tag{5}$$

With regard to oxygen standard electrode potential, as long as difference of cathodic and anodic standard electrode potential values is negative, getting electron from it in order to form S^{2-} is impossible

$$O_2 + 4H^+ + 4e \leftrightarrows 2H_2O \quad E_0 = 1.20\,V \tag{6}$$

$$S + 2e \leftrightarrows S^{2-} \quad E_0 = 0.14\,V \tag{7}$$

During the precipitation of Sb_2S_3, the conditional electrode potential equals $E_0' = E_0 + 0.06\,Pksp$, and therefore a reaction of Sb^{3+} and S^{2-} with high rate rather than primary rate is done. As Sb_2S_3 is a narrow band gap semiconductor (Eg is 1.7 ev for bulk), with decreasing diameter to nanoscale, novel optical properties may be observed [18]. The photoluminescence (PL) spectrum of synthesized antimony sulfide, shown in Figure 5, has an excitation peak at 348 nm (Figure 5(a)), and the emission peak can be observed at 450, 500 nm (Figure 5(b)).

The UV/Vis spectrum (prepared by dispersion of Sb_2S_3 products in ethanol) shows an absorption band at 215 nm with band gap around 2.50 ev which indicates a blue-shift phenomenon, as commonly observed for nanomaterials (Figure 6).

Most of the materials have different structural defects that create defect energy levels between band gaps of material. These defects result in difference between the UV absorption and PL excitation spectra.

4. Conclusion

In summary, a redox reaction approach in hydrothermal condition has been developed to prepare Sb_2S_3 nanorods with high yield at 180°C and 24 h. The length of nanorods is up to 4 μm, and their diameter is around 50–140 nm. Using iodine as an initiator of oxidation-reduction reaction is reported for the first time. The formation mechanism of Sb_2S_3 based on redox reaction is proposed. In the current process, I_2 plays an important role in the formation of Sb_2S_3 nano materials, and other oxidizing agents can be worthwhile for preparing nanostructures in the future. As a common feature for nanomaterials, a blue shift was observed in the case of optical absorption.

Acknowledgments

This work is funded by the 2010 Yeungnam University Research Grant. Y. Hanifehpour thanks the Council of the University of Tabriz for their invaluable guidance.

References

[1] B. Roy, B. R. Chakraborty, R. Bhattacharya, and A. K. Dutta, "Electrical and magnetic properties of antimony sulphide (Sb_2S_3) crystals and the mechanism of carrier transport in it," *Solid State Communications*, vol. 25, no. 11, pp. 937–940, 1978.

[2] O. Savadogo and K. C. Mandal, "Studies on new chemically deposited photoconducting antimony trisulphide thin films," *Solar Energy Materials and Solar Cells*, vol. 26, no. 1-2, pp. 117–136, 1992.

[3] B. H. Juárez, M. Ibisate, J. M. Palacios, and C. López, "High-energy photonic bandgap in Sb_2S_3 inverse opals by sulfidation processing," *Advanced Materials*, vol. 15, no. 4, pp. 319–322, 2003.

[4] N. K. Abrikosov, V. F. Bankina, L. Poretakaya, and L. E. Shelimova, *Semiconducting II–VI and V–VI Compounds*, Plenum, New York, NY, USA, 1969.

[5] D. Arivuoli, F. D. Gnanam, and P. Ramasamy, "Growth and microhardness studies of chalcogneides of arsenic, antimony and bismuth," *Journal of Materials Science Letters*, vol. 7, no. 7, pp. 711–713, 1988.

[6] C. N. Rao, F. L. Deepak, and G. Gundiah, "Inorganic nanowires," *Progress in Solid State Chemistry*, vol. 31, no. 1-2, pp. 5–147, 2003.

[7] Z. R. Geng, M. X. Wang, G. H. Yue, and P. X. Yan, "Growth of single-crystal Sb_2S_3 nanowires via solvothermal route," *Journal of Crystal Growth*, vol. 310, no. 2, pp. 341–344, 2008.

[8] S. R. Messina, M. T. Nair, and P. K. Nair, "Solar cells with Sb_2S_3 absorber films," *Thin Solid Films*, vol. 517, no. 7, pp. 2503–2507, 2009.

[9] H. M. Yang, X. H. Su, and A. D. Tang, "Microwave synthesis of nanocrystalline Sb_2S_3 and its electrochemical properties," *Materials Research Bulletin*, vol. 42, no. 7, pp. 1357–1363, 2007.

[10] M. Lalla-Kantouri, A. G. Marison, and G. E. Manoussakis, "Thermal decomposition of tris(*N, N*-disubstituteddithiocarbamate) complexes of As(III), Sb(III) and Bi(III)," *Journal of Thermal Analysis and Calorimetry*, vol. 29, no. 5, pp. 1151–1169, 1984.

[11] J. Yang, H. Zeng, S. H. Yu, L. Yangand, and Y. H. Zhang, "Pressure-controlled fabrication of stibnite nanorods by the solvothermal decomposition of a simple single-source precursor," *Chemistry of Materials*, vol. 12, no. 10, pp. 2924–2929, 2000.

[12] W. J. Lou, M. Chen, X. B. Wang, and W. M. Liu, "Novel single-source precursors approach to prepare highly uniform Bi_2S_3 and Sb_2S_3 nanorods via a solvothermal treatment," *Chemistry of Materials*, vol. 19, no. 4, pp. 872–878, 2007.

[13] Y. Yu, R. H. Wang, Q. Chen, and L. M. Peng, "High-quality ultralong Sb_2S_3 nanoribbons on large scale," *Journal of Physical Chemistry B*, vol. 109, no. 49, pp. 23312–23315, 2005.

[14] C. Li, X. G. Yang, Y. F. Liu, Z. Y. Zhao, and Y. T. Qian, "Growth of crystalline Sb_2S_3 nanorods by hydrothermal method," *Journal of Crystal Growth*, vol. 255, no. 3-4, pp. 342–347, 2003.

[15] X. Zheng, Y. Xie, L. Zhu, X. Jiang, Y. Jia, and W. Song, "Growth of Sb_2E_3 (E = S, Se) polygonal tubular crystals via a novel solvent-relief-self-seeding process," *Inorganic Chemistry*, vol. 41, no. 3, pp. 455–461, 2002.

[16] Y. T. Qian, K. Tang, C. Wang, and G. Zhou, "Antimony sulfide tetragonal prismatic tubular crystals," *Journal of Materials Chemistry*, vol. 11, no. 2, pp. 257–259, 2009.

[17] X. Wang, J. Zhuang, Q. Peng, and Y. Li, "A general strategy for nanocrystal synthesis," *Nature*, vol. 437, no. 7055, pp. 121–124, 2005.

[18] A. M. Qin, U. P. Fang, and W. X. Zhao, "Directionally dendritic growth of metal chalcogenide crystals via mild template-free solvothermal method," *Journal of Crystal Growth*, vol. 283, no. 1-2, pp. 230–241, 2005.